Characterization of Crosslinked Poly(vinyl alcohol)-Based Membranes with Different Hydrolysis Degrees for Their Use as Electrolytes in Direct Methanol Fuel Cells

A. Martínez-Felipe,[1] C. Moliner-Estopiñán,[1] C. T. Imrie,[2] A. Ribes-Greus[1]

[1]*Institute of Materials Technology, Universidad Politécnica de Valencia, Camino de Vera s/n, 46022, Valencia, Spain*
[2]*Department of Chemistry School of Natural and Computing Sciences, University of Aberdeen, Aberdeen, AB24 3UE, Scotland, United Kingdom*

Received 30 November 2010; accepted 22 June 2011
DOI 10.1002/app.35138
Published online 11 October 2011 in Wiley Online Library (wileyonlinelibrary.com).

ABSTRACT: The effect of the degree of hydrolysis of poly(vinyl alcohol) (PVA) substrates on the preparation and properties of crosslinked membranes prepared via esterification with sulfosuccinic acid (SSA) has been studied using attenuated total reflectance—Fourier transform spectroscopy (ATR–FTIR) and thermogravimetric analysis (TGA). Three PVA substrates with degrees of hydrolysis of 89, 96, and 99% were crosslinked using SSA at high temperatures. FTIR spectroscopy revealed that esterification occurred in all the membranes and to some extent, prior to heat treatment. The final morphology of the membranes was dependent on both the SSA concentration and the composition of the PVA substrate. Thermogravimetric analysis showed an increase in the thermal stability of the PVA-SSA membranes with respect to their PVA substrates arising from the formation of a crosslinked structure. In addition, TGA revealed the presence of free and tightly bound water in the PVA-SSA membranes. Thermal treatment had a more pronounced effect on the properties of the PVA substrates having higher degrees of hydrolysis. The results from the swelling tests, the ionic exchange capacities (IEC) and the tests in DMFC monocells demonstrated that a balance between water and methanol selectivity and ionic conduction determines the potential of these materials to act as electrolytes in fuel cells. © 2011 Wiley Periodicals, Inc. J Appl Polym Sci 124: 1000–1011, 2012

Key words: crosslinking; FTIR; thermogravimetric analysis (TGA); polymer synthesis and characterization; renewable resources

INTRODUCTION

Direct methanol fuel cells (DMFC) have considerable technological potential as an alternative power source, particularly for portable applications, which arises from a combination of environmental and sustainability issues, as well as liquid methanol at room temperature providing a higher energy density when compared to technologies such as lithium ion batteries.[1–3] An individual DMFC cell comprises of three main elements: an anode (where the oxidation of methanol takes place), a cathode (where the reduction of oxygen occurs), and a polymeric electrolyte membrane separating them (PEM). The PEM must control mixing between the methanol and oxygen and also facilitate proton conduction from the anode to cathode, so completing the electrochemical reactions.[4] A major challenge in the development of DMFCs is the so-called crossover phenomenon in which unreacted methanol diffuses through the PEM and which can reduce the cell's efficiency by as much as 30%. In response to this challenge, intense research has focused on the design of new materials having improved transport properties compared to the commercial membranes presently used as electrolytes in fuel cells, such as Nafion.[5] The aim of this work is to prepare materials with structures that combine high water contents to facilitate and promote proton conductivity with low methanol permeability to avoid fuel crossover.[6] To achieve this goal in a rational manner, we must both understand the morphology of the membrane, and learn how to control several parameters such as the interactions between functional groups, the organization of absorbed water, the extent of hydrogen bonding, and the chemical environment of the proton conducting groups.

Poly(vinyl alcohol) (PVA)-based membranes have been studied in recent years as an alternative to commercial materials in DMFCs to avoid crossover because of their high selectivity for water with respect to alcohols.[5,7,8] Poly(vinyl alcohol) (PVA) is a nonionic, water-soluble polymer and the high concentration of OH groups along the polymer

Correspondence to: A. Ribes-Greus (aribes@ter.upv.es).
Contract grant sponsor: Spanish Ministry of Science and Innovation; contract grant numbers: ENE2007-67584-C03, UPOVCE-3E-013.
Contract grant sponsor: Spanish Ministry of Science and Innovation; contract grant numbers: ENE2007-67584-C03, UPOVCE-3E-013, IT2009-0074, FPI (2005), FPU (2005).
Contract grant sponsor: Generalitat Valenciana; contract grant number: Grisolia and Forteza 2010 and 2011.

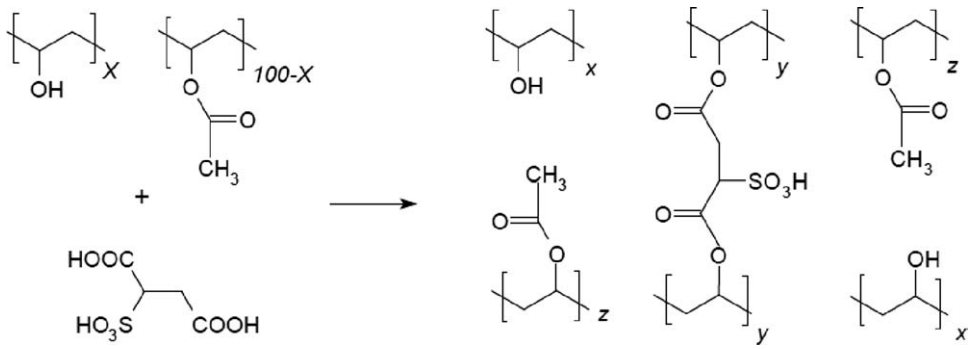

Figure 1 The reaction of PVA (a) and SSA (b) to produce the PVA-SSA membranes. The final proportions of the repeating units (x, y, and z) depend on the hydrolysis degree (X) and reaction conditions.

backbone endows PVA with a strong hydrophilic character and inter and intra molecular hydrogen bonding determines the morphology of the membranes. PVA is commercially prepared by hydrolysis of poly(vinyl acetate) (PVAc). The number of hydroxyl groups in the resulting PVA is used to define the hydrolysis degree (HD), which usually varies from 70 to 99% in commercial PVA.[9] To obtain membranes with good proton conductivity and enhanced mechanical stability, PVA membranes are usually crosslinked by agents containing ionic groups.

In this article, we study the effects of varying the PVA substrate, the sulfosuccinic acid (SSA) concentration and thermal treatment on the preparation and properties of PVA-SSA membranes having application potential in DMFC technologies. Different PVA-SSA membranes were prepared by varying the hydrolysis degree of the PVA substrate (HD = 89, 96, and 99%) and the concentration of SSA in the range 0–30% (SSA weight percentage). The degree of hydrolysis of the PVA substrate has been varied because this will effect the crosslinking reactions with SSA and will also influence the hydrophilic character of the resulting membranes. Fourier transform infrared spectroscopy (FTIR) and thermogravimetric analysis (TGA) have been used to study the molecular interactions between the components of the membranes and their thermal stability. The structure of the PVA-SSA crosslinked materials is shown in Figure 1. By the introduction of sulfonic groups, the resulting membranes show enhanced proton conductivities as well as increased thermal and mechanical stability arising from the formation of a 3D interconnected network.[10–12] The study is completed with the study of the water and methanol absorption through swelling tests, the calculation of ionic exchange capacity (IEC) and the acquisition of the polarization (I–V) curves in DMFC monocells of some of the PVA-SSA membranes.

EXPERIMENTAL PROCEDURE

Materials

Three samples of poly(vinyl alcohol) (PVA) with different hydrolysis degrees (89% hydrolyzed, MW = 85,000–124,000 g mol^{-1}; 96% hydrolyzed, MW = 85,000–146,000 g mol^{-1}; 99% hydrolyzed, MW = 85,000–124,000 g mol^{-1}) and a commercial sulfosuccinic acid (SSA) solution (70%, weight % in H_2O) were purchased from Sigma-Aldrich.

Membrane preparation

Three series of membranes were prepared based on PVA substrates with hydrolysis degrees of 89, 96, and 99%. All the membranes were prepared following the same procedure shown in Figure 1. Thus, PVA was dissolved in distilled water by stirring at 90°C for 6 h to give a 10% (weight %) solution. After cooling, the commercial SSA solution was added and the mixture stirred at room temperature for 1 day. The amount of the commercial SSA solution added varied to form PVA-SSA membranes containing 5, 10, 15, 20, 25, and 30% by weight percentage of SSA with respect to PVA. The resulting solutions were cast on a Teflon sheet and water was removed by drying to constant weight in ambient conditions to give the untreated PVA-SSA membranes. These membranes were heated at 110°C for 2 h to obtain the heat-treated PVA-SSA membranes.

The membranes are referred to using the code, PVAXhyd$Y$%, in which X is the hydrolysis degree of the PVA substrate (HD) and Y the weight percentage of SSA used in the crosslinking reaction. Membranes consisting of the three PVA substrates containing no crosslinking agent were also prepared as the control experiment.

Attenuated total reflectance—Fourier transform infrared spectroscopy (ATR-FTIR)

The FTIR experiments were performed using a Thermo Nicolet 5700 spectrometer (MA, Waltham) with an ATR accessory. The samples were placed on a diamond crystal, and the experiments were performed using one bounce and an incident angle of 45°C. The spectra were collected after 128 scans with an accuracy of 4 cm^{-1}. Background spectra were

collected before each series of experiments. All the experiments were performed three times and the average was calculated.

Thermogravimetric analysis (TGA)

The TGA thermograms were obtained using a Mettler Toledo TGA/SDTA 851 analyzer (OH, Columbus). Measurements were performed following a dynamic program from 25 to 700°C at a linear heating rate of 10°C min^{-1} under inert argon (Ar) atmosphere with a flow rate of 50 mL min^{-1}. Sample masses were around 5 mg. All the experiments were performed three times and the average was calculated.

Transport properties in DMFC

The absorption of water and methanol was evaluated by performing swelling tests on the PVA-SSA membranes at 35°C. Rectangular samples of 4 × 1 cm^2 were initially weighted ($t = 0$, w_0), using a Mettler Toledo balance (0.01 mg accuracy), and were submerged in test tubes containing water, methanol and 8% methanol aqueous binary mixture (wt %). The test tubes were placed in a thermostated SELECTA Ultrasonic bath (accuracy 0.1°C) at 35°C, to simulate the behavior of the materials at typical DMFC operating temperatures. The absorption of the solvents by the membranes was measured gravimetrically at different times (w_t), by extracting the samples from the test tubes and carefully removing the excess liquid from the films with a tissue. The membranes were immersed in the solutions until no further gain weight was observed, to achieve equilibrium conditions. The swelling parameter at equilibrium (S_{eq}(%)) was calculated by the following expression:

$$S_{eq}(\%) = \frac{w_{eq} - w_0}{w_0} \cdot 100,$$

where w_{eq} is the weight of the sample at equilibrium.

On the other hand, the ionic exchange capacity (IEC) was calculated by a titration method. Samples of the membranes were submerged in a 0.1*N* NaOH solution during 24 h to promote exchange of the protons from the SO_3H groups of SSA. About 10 mL of the resulting NaOH solution were then valorized by a standard 0.1*N* HCl solution, using phenoftalein as the indicator. The IEC (meq g^{-1}) was calculated by using the following expression:

$$\mathrm{IEC} = \frac{\mathrm{meq(NaOH_0)} - \mathrm{meq(NaOH_{eq})}}{w_0} (\mathrm{meq/g})$$

where meq($NaOH_0$) and meq($NaOH_{eq}$) are the miliequivalents (meq) of NaOH calculated before and after submerging the samples, respectively, and w_0 is the weight of the dry sample.

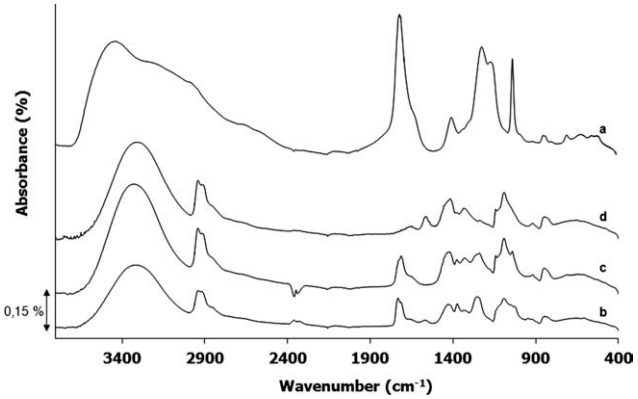

Figure 2 FTIR spectra of the pure components: (a) SSA commercial solution; PVA substrates: (b) PVA89hyd0%, (c) PVA96hyd0%, (d) PVA99hyd0%.

The preliminary behavior of the new membranes in fuel cells was studied by tests on DMFC monocells at room temperature. A F107 PEMFC KIT (provided by H-Tec Wasserstoff-Energie-Systeme GmbH, Luebeck, Gernany) was used to acquire the I–V polarization curves of selected membranes. The anode was continuously supplied with a liquid methanol aqueous solution while air was pumped at the cathode at a flow rate of 3.5 L h^{-1}. The electrodes consisted on flat carbon cloths impregnated with Pt as the catalyzer. Square PVA-SSA membranes (4 × 4 cm^2) were placed between the two electrodes after equilibrating during 30 min, and the I–V curves (polarization curves) were obtained by varying the charge applied to the cell.

RESULTS AND DISCUSSION

Characterization of the pure components

Figure 2 shows the FTIR spectra of the commercial SSA solution and the PVA substrates with different hydrolysis degrees. The assignments of the main absorption bands are listed in Table I. The FTIR curve of SSA [Fig. 2(a)] shows several bands in the O—H stretching region (ν = 3000–3600 cm^{-1}) associated with the carboxylic acid groups (COOH) and water molecules. The prominent peak in the vicinity of 1043 cm^{-1} indicates the presence of SO_3^- groups obtained by dissociation of the SO_2OH groups of the SSA molecules. The high water content in the solution is also evident from the H_2O bending band at ~ 1650 cm^{-1} region and which overlaps the C=O stretching band at ν = 1724 cm^{-1}.

The FTIR spectra of the three PVA substrates [Fig. 2(b–d)] contain several characteristic bands,[13,14,16–20] specifically: the OH stretching vibration (ν_{OH} = 3000–3600 cm^{-1}) and OH out of plane deformation

TABLE I
Assignments of the Main FTIR Absorption Bands of the PVA Membranes

Region (cm^{-1})	Assignment	Contributions	References
3400–3000	OH stretching	Intermolecular hydrogen bonding PVA, H_2O, SSA	[13, 14, 17, 21]
1660–1640	OH bending	H_2O	
920	OH out of plane	Carboxylic group SSA	
2910–2950	CH_2 stretching	PVA structure, SSA	[13]
1420	CH_2 scissoring		
1330	CH_2 deformation		
850	CH_2 rocking		
1790–1660	C=O stretching	Acetate groups PVA, carboxyl groups SSA	[13, 20, 21]
1250	C—O stretching	Acetate groups PVA, SSA	
1140	C—O stretching	Crystalline form	
1090	C—O stretching	Acetate groups PVA, SSA	
1040	SO_3^- stretching	SO_3^- group SSA	[12]

($\nu = 920\ cm^{-1}$)[13–15]; the deformation vibration of the CH_3 groups ($\nu = 1340\ cm^{-1}$)[12]; the C—O stretching vibration of the alcohol groups ($\nu = 1140\ cm^{-1}$ (crystalline) and $\nu_{COH} = 1090\ cm^{-1}$)[16]; the bending vibration of the water molecules ($\nu_{H2O} = 1650\ cm^{-1}$) associated with PVA. We note that the hydroxyl groups of water also contribute to the OH stretching band at 3600–3000 cm^{-1}.[15,18] In the PVA substrates with lower hydrolysis degrees (PVA89hyd and PVA96-hyd) it is also possible to identify the bands associated with the acetate groups at $\nu_{C=O} = 1730\ cm^{-1}$ (C=O stretching) and $\nu_{COC} = 1250\ cm^{-1}$ (C—O—C stretching).[15]

The maximum absorbance and wavenumber of the bands associated with the hydroxyl (Abs_{3300}, ν_{OH}), carboxyl (Abs_{1720}, $\nu_{C=O}$), and sulfonate groups (Abs_{1040}, ν_{SO3}) have been calculated.[21] The values of absorbance were normalized with respect to the stretching vibration band of the CH_2 groups of the polymer backbone ($\nu = 2940\ cm^{-1}$), thus:

$$I_{OH} = \frac{Abs_{3300}}{Abs_{2940}}$$

$$I_{C=O} = \frac{Abs_{1720}}{Abs_{2940}}$$

$$I_{SO_3} = \frac{Abs_{1040}}{Abs_{2940}}$$

and the results are summarized in Table II. The increased hydrolysis of acetate groups to give hydroxyl groups, causes a reduction of the C=O band ($I_{C=O}$) on increasing hydrolysis degrees, while conversely the absorbance of the O—H band is greatest for PVA99hyd0% reflecting that this contains the highest concentration of hydroxyl groups. It should be noted that the different O—H concentrations in these samples give rise to shifts in the position of other IR bands due to the formation of hydrogen bonds of differing strengths.[22,23]

The thermal stabilities of the PVA substrates and SSA have also been studied. The derivative thermogravimetric (DTG) curves of the SSA commercial solution and the three PVA substrates are shown in Figure 3. The DTG curve of SSA [Fig. 3(a)] shows a mass loss peak at 100°C, which is attributed to the loss of water, and a main decomposition process in the region 200–330°C, related to the desulfonation process. The degradation of PVA proceeds in, at least, three steps [Fig. 3(b–d)]. At low temperatures ($T_1 = 100$°C) a low intensity peak is observed which can be attributed to the loss of water (Process 1). In the 200–400°C region, a strong peak is seen which is assigned to the loss of OH groups and to the deacetylation of the PVA chains (Process 2). Finally, a weaker process is observed in the 400–500°C region which is attributed to the degradation of the polymeric backbone (Process 3). The results are in agreement with those reported in the literature.[6,24,25]

The temperature at the maximum degradation rate (T_i) and the mass loss ($\Delta\omega_i$) associated with the three main decomposition processes (Processes i = 1, 2, and 3) observed for the PVA substrates are plotted in Figure 4 as a function of the hydrolysis

TABLE II
Position and Absorption Parameters of the Characteristic IR Bands Observed in the Spectra of the PVA Membranes

Sample	OH st		C=O st		SO_3^- st	
	υ_{OH} (cm^{-1})	I_{OH}	$\upsilon_{C=O}$ (cm^{-1})	$I_{C=O}$	υ_{SO3} (cm^{-1})	I_{SO3}
SSA	3435	1.376	1724	1.936	1042	1.284
PVA89hyd0%	3319	1.683	1732	0.817	–	–
PVA96hyd0%	3307	1.512	1716	0.333	–	–
PVA99hyd0%	3334	1.821	–	–	–	–

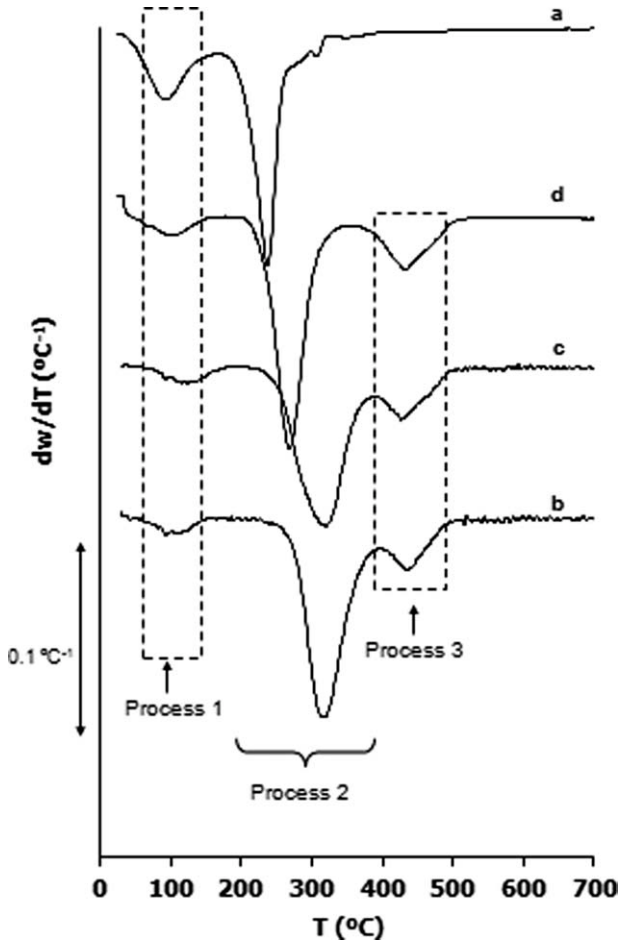

Figure 3 Derivative thermogravimetric (DTG) curves of: (a) commercial SSA solution; the PVA substrates: (b) PVA89hyd0%, (c) PVA96hyd0%, (d) PVA99hyd0%.

degree. As expected, there is an increase in the water absorbed ($\Delta\omega_1$) by the PVA substrates on increasing the hydrolysis degrees due to the higher concentration of hydrophilic OH groups in the PVA chain.[8,16] The mass loss associated with Process 2 ($\Delta\omega_2$) decreases at high hydrolysis degrees (PVA99-hyd), presumably reflecting the conversion of CH_3COO groups into lighter OH groups during hydrolysis. This is also accompanied by a decrease in the temperatures of the degradation peak (T_2), which indicates that the acetate groups have higher thermal stability than the hydroxyl groups in PVA.[25] Finally, there is a slight decrease in the residual values on increasing hydrolysis degree. This implies that the decomposition of the PVA backbone is somehow promoted in samples containing higher OH concentrations.

Characterization of the PVA-SSA membranes before thermal treatment

The FTIR spectra of the PVA–SSA membranes were measured prior to thermal treatment. The IR spectra corresponding to the PVA99hyd series are shown in

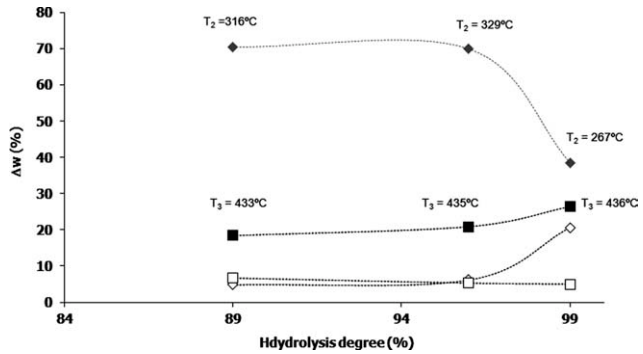

Figure 4 Weight losses associated with the degradation processes observed for the PVA substrates as a function of the hydrolysis degree: (◇) water loss ($\Delta\omega_1$); (◆) side group decomposition ($\Delta\omega_2$); (■) main chain decomposition ($\Delta\omega_3$); (□) residual at 700°C.

Figure 5, which also includes the spectrum of the corresponding PVA membrane (PVA99hyd0%). The FTIR spectra of the PVA-SSA membranes show a number of differences when compared to that of PVA as a result of the addition of SSA. A new band is seen at around $\nu_{SO3} = 1040\ cm^{-1}$ in the spectra of the PVA-SSA membranes, confirming the presence of the sulfonate groups which will act as proton conducting groups in the PVA-SSA membranes. Changes are seen in the O—H and C=O regions of the spectra for all three series.

To quantify some of these changes involving characteristic bands in the spectra of the PVA-SSA membranes, the maximum absorbance of the OH, C=O, and SO_3^- bands were calculated for all the samples before being submitted to thermal treatment. These were normalized with respect to the stretching vibration of the CH_2 group ($\nu = 2940\ cm^{-1}$) to obtain I_{OH}, $I_{C=O,}$ and I_{SO3}, following the procedure

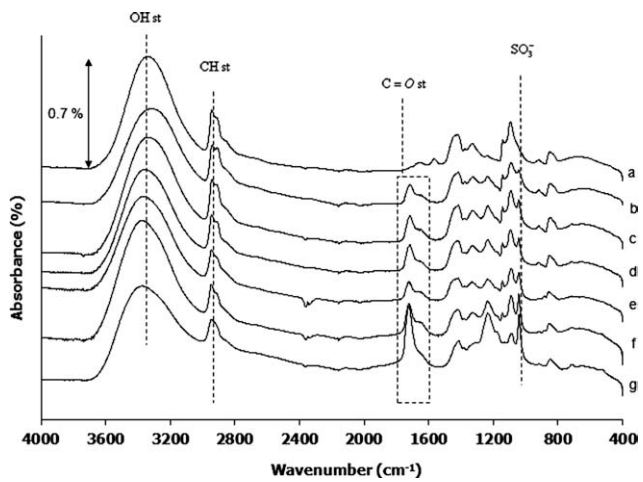

Figure 5 FTIR spectra of the 99hydPVA–SSA membranes before thermal treatment: (a) PVA99hyd0%, (b) PVA99-hyd5%, (c) PVA99hyd10%, (d) PVA99hyd15%, (e) PVA99-hyd20%, (f) PVA99hyd25%, (g) PVA99hyd30%.

TABLE III
Position and Absorption Parameters of the Characteristic IR Bands Observed in the Spectra of the *PVA89hyd* PVA-SSA Membranes Before (Untreated; U-T) and After (Treated; T) Heat Treatment

	υ_{OH} (cm^{-1})	I_{OH}	$\upsilon_{C=O}$ (cm^{-1})	$I_{C=O}$	υ_{SO3} (cm^{-1})	I_{SO3}
C_{SSA} (wt %)	Untreated → treated	U-T → T	U-T → T	U-T → T	U-T → T	U-T → T
0	3319	1.68	1732	0.82		–
5	3334 → 3369	1.75 → 1.38	1713 → 1716	0.57 → 0.90	1043 → 1039	0.67 → 0.89
10	3349 → 3341	1.80 → 1.34	1732 → 1715	0.89 → 0.73	1042 → 1039	0.70 → 0.71
15	3336 → 3376	1.60 → 1.21	1714 → 1722	0.94→ 0.95	1041 →1039	0.88 →0.92
20	3308 → 3370	1.45 → 1.10	1714 → 1716	0.74 → 1.08	1039 → 1038	0.76→ 1.11
25	3360 → 3392	1.66 → 1.09	1723 → 1716	0.84 → 1.16	1041 → 1038	0.88 → 0.89
30	3344→ 3370	1.46 → 0.74	1716 → 1727	0.93 → 0.89	1039 → 1035	0.93 → 0.85

described earlier for the PVA substrates. These data are shown in Tables III–V for the PVA89hyd, PVA96hyd, and PVA99hyd series, respectively. The frequencies of the peak maxima associated with these bands are also listed in Tables III–V.

As expected, there is an increase in the SO_3^- band at higher concentrations of SSA in the PVA-SSA membranes. The analysis of this band is complicated, however, by the presence of the prominent peak corresponding to the C—OH stretching band (ν_{COH} = 1090 cm^{-1}) of the PVA backbone. The introduction of SSA in the membranes is also accompanied by an increase in the C=O stretching band, and this is particularly evident for the PVA96hyd and PVA99hyd series (see Table V). This is attributed to the presence of the carboxylic groups present in the SSA molecules.[26,27] For the PVA99hyd samples (see Table V), the band associated with the acetate groups of PVA is very weak, and it is apparent that the band associated with the C=O groups of the SSA molecules appears at lower frequencies than in the SSA commercial solution ($\nu_{C=O}$ = 1724 cm^{-1}). It is also noteworthy that this band shifts to higher wavenumbers as the concentration of SSA, C_{SSA}, increases in the membranes. These results suggest that the SSA carboxyl groups may be forming stronger interactions with the PVA OH groups than with other SSA molecules.

The formation of such interactions between SSA and PVA is also reflected in the frequencies listed for the O—H stretching band in Tables III–V. The peak maximum of the IR band associated with the hydroxyl groups of PVA shifts to higher frequencies in the PVA-SSA membranes, indicating the formation of less energetic interactions in the presence of SSA molecules. A detailed analysis of the nature of the hydrogen bonding involved would be highly complex due to the presence of several hydrogen bond donors and acceptors (O—H, COOH, SO_3^-). In addition, some of the changes in this region of the spectra are likely to be overlapped by the presence of bands associated with water, and furthermore, water could act as a plasticizer via the formation of new intermolecular hydrogen bonds. This is particularly evident in the high frequency associated with the band in the spectrum of the SSA commercial solution (ν = 1724 cm^{-1}), which contains 70% of water (wt %). All these effects are more apparent in the series with higher hydrolysis degrees (PVA96-hyd and PVA99hyd).

The thermal stability of the PVA–SSA membranes prior to thermal treatment was studied by TGA. Figure 6 shows the DTG curves for the PVA96hyd series, and similar results were obtained for the other series. The most notable change observed when compared to the DTG curves of the PVA substrates is the appearance of a very strong weight loss peak in the 100–200°C region in all the PVA-SSA membranes. This peak (T_1, Region 1 in Fig. 6)

TABLE IV
Position and Absorption Parameters of the Characteristic IR Bands Observed in the Spectra of the *PVA96hyd* PVA-SSA Membranes Before (Untreated; U-T) and After (Treated; T) Heat Treatment

	υ_{OH} (cm^{-1})	I_{OH}	$\upsilon_{C=O}$ (cm^{-1})	$I_{C=O}$	υ_{SO3} (cm^{-1})	I_{SO3}
C_{SSA} (wt %)	Untreated → treated	U-T → T	U-T → T	U-T → T	U-T → T	U-T → T
0	3307	1.51	1716	0.33	–	–
5	3354 → 3314	2.07 → 1.53	1712 → 1718	0.27 → 0.35	1042 → 1039	0.65 → 0.43
10	3333 → 3347	1.67 → 1.39	1714 → 1713	0.57 → 0.79	1040 → 1038	0.19 → 0.74
15	3401 → 3365	2.62 → 1.28	1722 → 1716	0.33 → 0.85	1041 → 1039	0.76 → 0.84
20	3345 → 3373	1.76 → 1.35	1716 → 1716	0.66 → 0.85	1041 → 1038	0.95 → 0.92
25	3365 → 3366	1.57 → 1.30	1716 → 1716	0.97 → 0.87	1041 → 1039	0.84 → 0.86
30	3354 → 3382	1.69 → 1.20	1716 → 1716	0.80 → 0.83	1042 → 1039	0.65 → 0.81

TABLE V
Position and Absorption Parameters of the Characteristic IR Bands Observed in the Spectra of the *PVA99hyd* PVA-SSA Membranes Before (Untreated; U-T) and After (Treated; T) Heat Treatment

	υ_{OH} (cm^{-1})	I_{OH}	$\upsilon_{C=O}$ (cm^{-1})	$I_{C=O}$	υ_{SO3} (cm^{-1})	I_{SO3}
C_{SSA} (wt %)	Untreated → treated	U-T → T	U-T → T	U-T → T	U-T → T	U-T → T
0	3334	1.82	–	–	–	–
5	3308 → 3307	1.56→ 1.43	1715 → 1715	0.40 → 0.34	1042 → 1043	0.62 → 0.71
10	3334 → 3307	1.65 → 1.40	1716 → 1716	0.46 → 0.51	1043 → 1040	0.70 → 0.63
15	3354 → 3306	1.69 → 1.32	1716 → 1715	0.54 → 0.43	1043 → 1039	0.65 → 0.58
20	3364 → 3306	1.81 → 1.33	1723 → 1716	0.50 → 0.52	1042 → 1040	0.65 → 0.81
25	3378 → 3353	1.98 → 1.37	1723 → 1728	0.70 → 0.82	1042 → 1040	0.85 → 0.92
30	3376 → 3372	1.51 → 1.11	1724 → 1728	1.19 → 1.28	1041 → 1039	1.07 → 1.10

has been attributed to the existence of water tightly bound to the polymer structure and also to the water produced by esterification reactions.[14,28] The presence of bound water in the PVA-SSA membranes is very important to ensure proton conductivity in these potential DFMC electrolytes by the creation of ionic clusters which facilitate proton conduction. In the DTG curves shown in Figure 6, it is also possible to observe a low temperature shoulder on this peak (T = 100°C) which indicates the presence of free water. Some weak processes are also visible in the 200–320°C temperature region (T_2, Region 2) which may be attributed to desulfonation, and also to the loss of OH and acetate groups from the polymer.[14,28]

The degradation process associated with the main chains in the PVA-SSA membranes (T_3, Region 3) is more pronounced in the DTG curves for the PVA-SSA membranes compared to those of the PVA substrates. This also occurs for the residual values at 700°C, which increases from 5 to 7% (in the PVA substrates) to the 23 to 30% range (in the PVA-SSA membranes). These changes in the thermal degradation of the backbone and the residual values can be explained by the formation of a crosslinked structure by esterification occurring even before the membranes are submitted to the thermal treatment. This fact is consistent with the increase in the intensity of the C=O band in the FTIR spectra described earlier.[14,25,26] Although the DTG curves of all the three

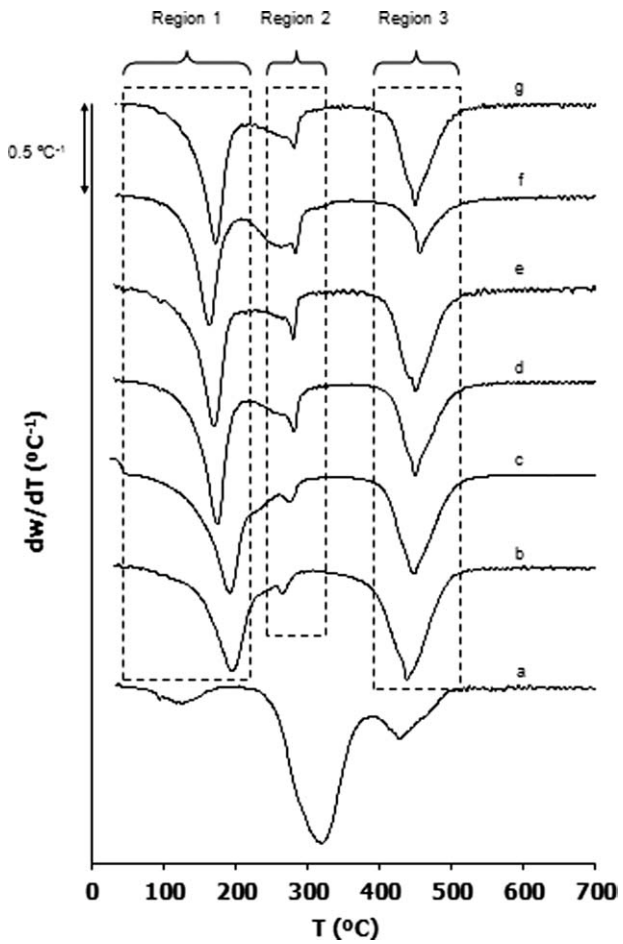

Figure 6 DTG curves of the 96hydPVA–SSA membranes before thermal treatment: (a) PVA96hyd0%, (b) PVA96-hyd5%, (c) PVA96hyd10%, (d) PVA96hyd15%, (e) PVA96-hyd20%, (f) PVA96hyd25%, (g) PVA96hyd30%.

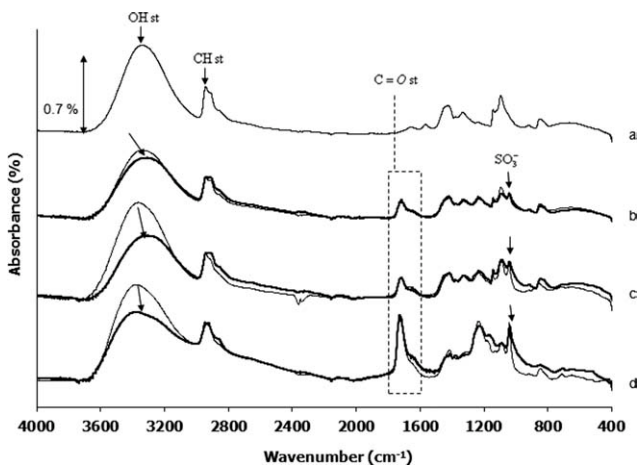

Figure 7 FTIR curves of the 99hydPVA–SSA membranes before (thin lines) and after (thick lines) thermal treatment: (a) PVA99hyd0%, (b) PVA99hyd10%, (c) PVA99hyd20%, (d) PVA96hyd30%.

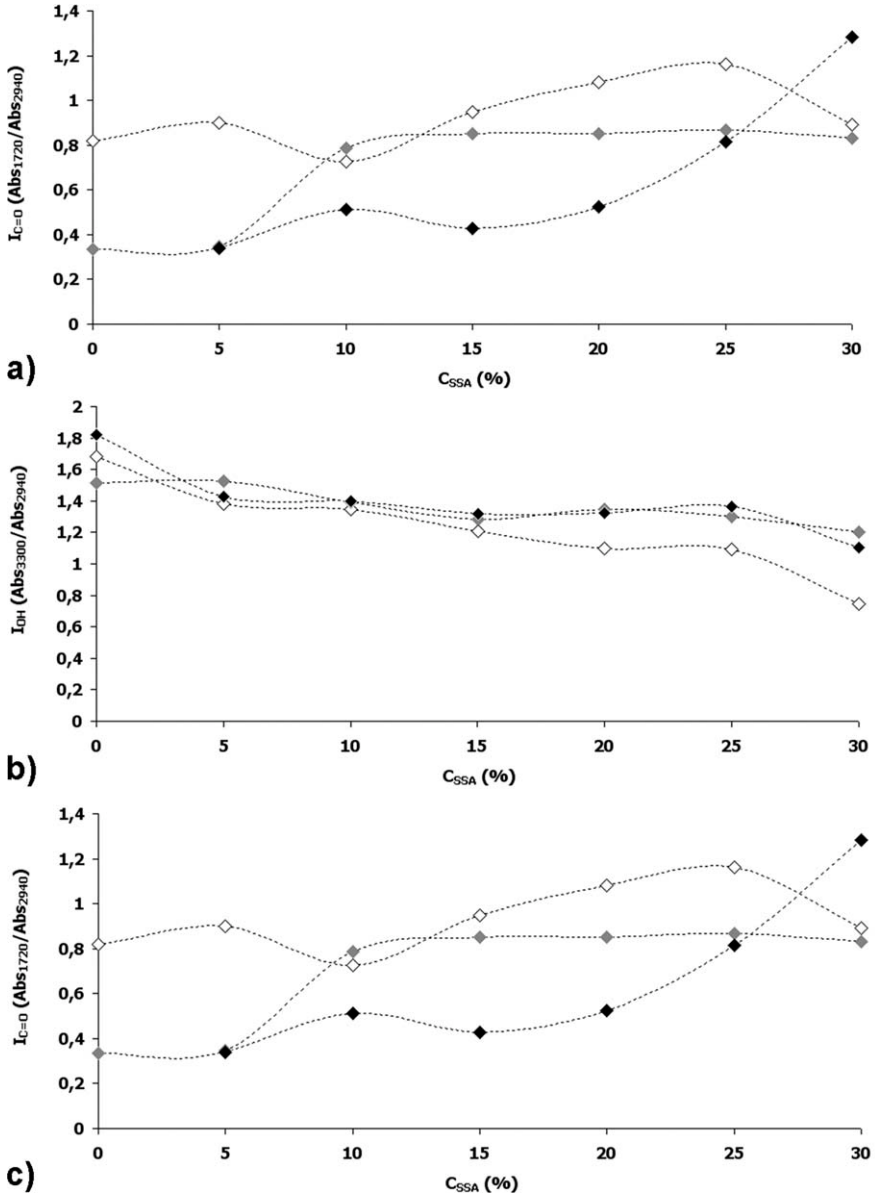

Figure 8 Relative IR absorbances of: (a) hydroxyl (I_{OH}); (b) carbonyl ($I_{C=O}$); (c) sulfonate groups (I_{SO3}) with respect to the CH_3 vibration band at 2940 cm^{-1} of the PVA-SSA membranes. Results corresponding to: (◇) PVA89hyd, (◈) PVA96hyd and (◆) PVA99hyd series.

sets of PVA-SSA membranes are similar, the amount of water present and the residual values are greatest for the membranes with the highest hydrolysis degrees (PVA-SSA 99%hyd).

Characterization of the PVA-SSA membranes after the thermal treatment

Figure 7 shows the FTIR spectra of selected PVA-SSA membranes post thermal treatment from the PVA99hyd series. The spectra of the untreated membranes and of the PVA substrate have also been included for comparative purposes. It is clear that thermal treatment results in changes in the FTIR spectra of the PVA-SSA membranes, particularly in the O—H, C=O, and SO_3^- regions. To quantify these changes, the values of I_{OH} $I_{C=O,}$ and I_{SO3} were obtained for the thermally treated membranes as described earlier, and are listed in Tables III–V.

Thermal treatment results in a remarkable reduction in the intensity of the broad band in the 3600–3000 cm^{-1} region, see Figure 7 and Tables III–V. This indicates the removal of OH groups as a result of esterification reactions between PVA and SSA.[8,29,30] The I_{OH}, $I_{C=O,}$ and I_{SO3} values have been plotted as a function of the SSA concentration in the

PVA-SSA membranes in Figure 8. The values of I_{OH} [Fig. 8(a)] decrease at higher SSA contents, indicating a further reduction of the OH-group concentration reflecting higher levels of esterification. This reduction is least pronounced for the PVA89hyd series, and increases with higher hydrolysis degrees. These results indicate that the PVA substrate (and therefore the initial concentration of OH groups in the polymer) plays a significant role in the esterification process of the PVA-SSA membranes.

It is also interesting to note that the increase in intensity of the C=O and SO_3^- bands [Fig. 8(b,c)] seen for the PVA99hyd series is particularly marked at higher SSA concentrations (C_{SSA}[mtequ] 15%). This suggests that esterification is promoted by high concentrations of crosslinking agent. By contrast, PVA substrates having lower hydrolysis degrees appear to behave differently. The maximum relative intensities of the SO_3^- and C=O bands occur for C_{SSA} = 20–25%, suggesting that the esterification process is somehow inhibited at higher SSA concentrations in these substrates.

The effect of the thermal treatment on the stability of the PVA-SSA membranes was studied. Thus, the DTG curves obtained for the PVA96%hyd series are shown in Figure 9, and similar results were obtained for all the other series. The degradation of the PVA-SSA membranes is not significantly changed by thermal treatment, and similar degradation regions are observed as seen for the prethermal treatment membranes, see Figure 6. These results confirm that the main structure of the polymers persists during thermal treatment.

The effect of the hydrolysis degree of the PVA substrate on the thermal degradation of the different PVA-SSA crosslinked membranes was investigated. The values of d_w/dT_i, T_i, and $\Delta\omega_i$ relating to the different degradation regions (i = 1, 2, and 3) were obtained from the experimental DTG curves of all the PVA-SSA membranes. The average ($\Delta\omega_i$) values were calculated separately for the PVA substrates, the untreated PVA-SSA membranes, and the thermally treated PVA-SSA membranes and are shown in Figure 10 for all three series. The PVA-SSA membranes prepared using high hydrolysis degree substrates (PVA99hyd% and PVA96hyd%) show the most pronounced changes post thermal treatment. The most thermally stable PVA-SSA crosslinked membranes are those prepared from the highest hydrolysis degree PVA substrate (PVA99hyd%). However, the values of water content for the PVA99%hyd membranes are considerably lower than those seen for the crosslinked membranes obtained using lower hydrolysis degree PVA substrates (PVA96hyd and PVA89hyd).[16,25,26]

On the other hand, the effect of the SSA concentration on the thermal stability of the crosslinked membranes has also been studied. The values of T_2, T_3 and residual for each series are listed in Table VI. These data show that the thermal stability of the polymer chains in the PVA-SSA crosslinked membranes produced from low hydrolysis degrees PVA substrates (PVA89hyd and PVA96hyd) is greater for higher SSA concentrations.

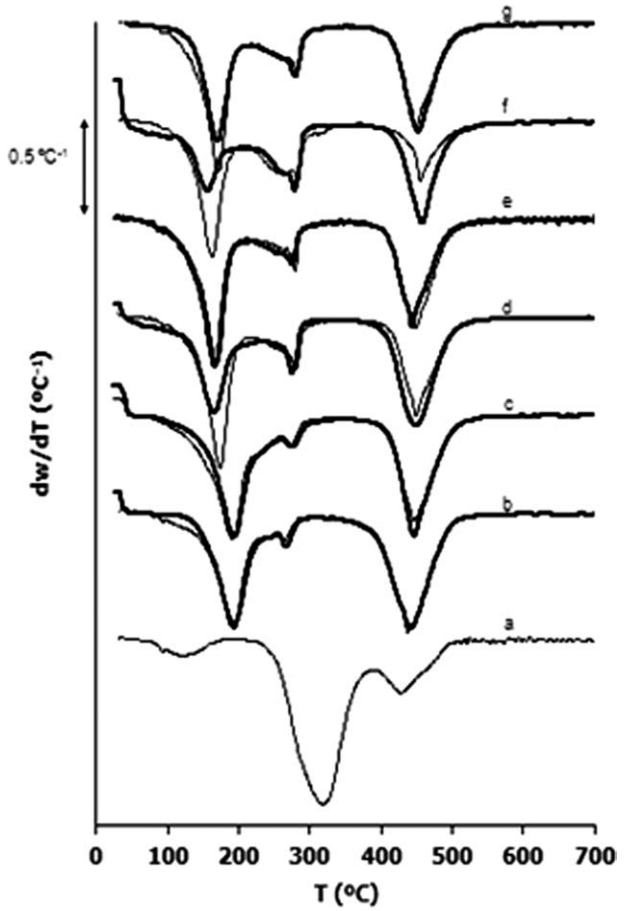

Figure 9 DTG curves of the 96hydPVA–SSA membranes after thermal treatment (thick lines): (a) PVA96hyd0%, (b) PVA96hyd5%, (c) PVA96hyd10%, (d) PVA96hyd15%, (e) PVA96hyd20%, (f) PVA96hyd25%, (g) PVA96hyd30% (thin lines).

These results suggest that PVA substrates with intermediate hydrolysis degrees can be the most convenient to control the structural parameters and water contents of PVA-SSA membranes through the addition of SSA crosslinking groups, possibly by a balance between physical and chemical crosslinking before and after thermal treatment.

Transport properties of the PVA-SSA membranes and tests in a DMFC monocells

In Figure 11 and Table VII we show the results from the swelling and IEC tests carried out to evaluate the future application of the PVA-SSA as membranes in fuel cells. The selected membrane was PVA96hyd

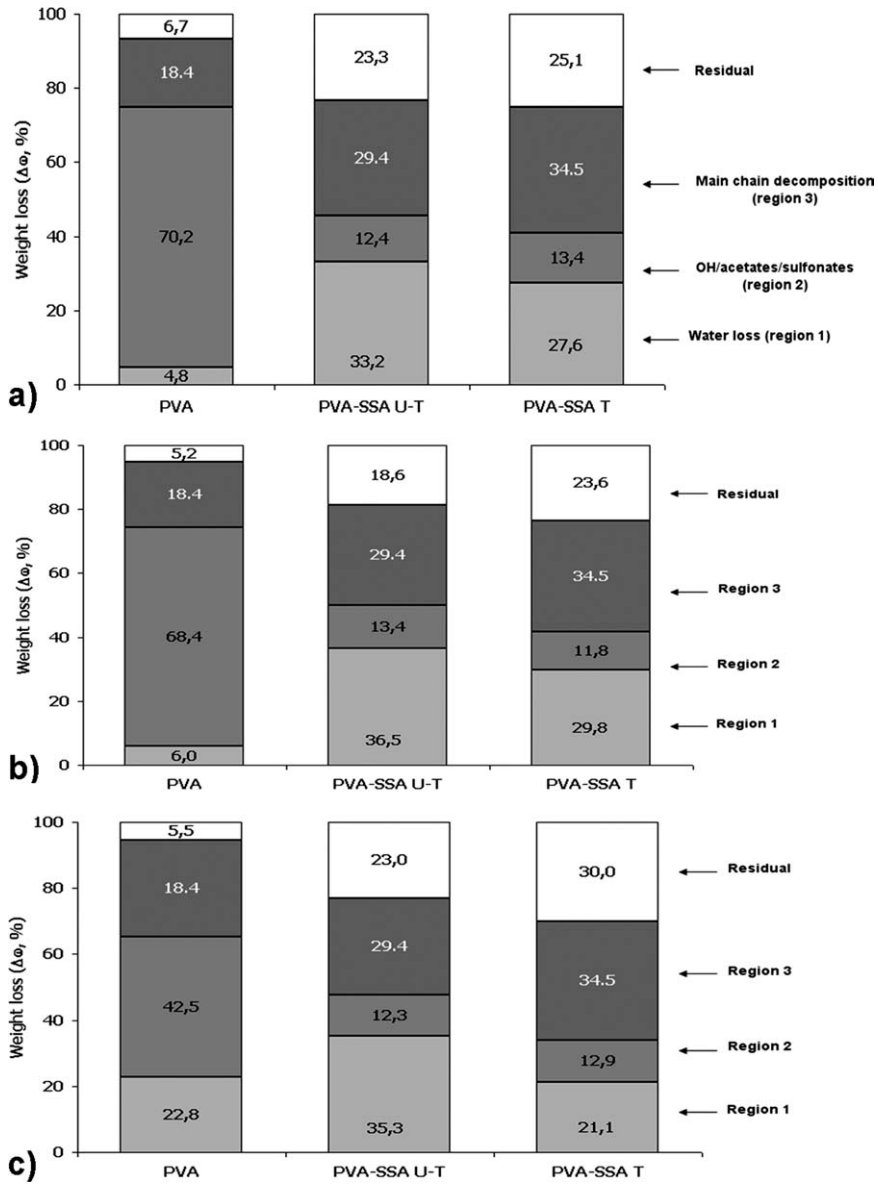

Figure 10 Average values of weight loss and residual for the decomposition of (a) 89hydPVA–SSA, (b) 96hydPVA–SSA, (c) 99hydPVA–SSA membranes. Left column corresponds to PVA substrates, central column to PVA-SSA membranes without thermal treatment (U-T) and right column to PVA-SSA membranes after thermal treatment (T).

because it presented the best performance as stated before. The membranes absorb more water than methanol, due to the high water/methanol selectivity of PVA-based materials.[5,7,8] Moreover, while the values of S_{eq}(%) decrease at increasing SSA concentrations in the samples submerged in water and its

TABLE VI
Parameters of the Thermal Decomposition of the PVA-SSA Membranes After Thermal Treatment

	89hyd			96hyd			99hyd		
C_{SSA} (wt %)	T_2 (°C)	T_3 (°C)	Residual (%)	T_2 (°C)	T_3 (°C)	Residual (%)	T_2 (°C)	T_3 (°C)	Residual (%)
0	317	436	6.7	329	436	5.3	267	433	5.0
5	248	447	21.3	266	442	22.1	274	448	30.4
10	274	447	26.1	274	446	20.4	267	448	33.6
15	277	452	26.0	274	449	22.0	278	448	36.3
20	277	453	27.3	277	451	23.0	272	447	30.2
25	278	453	26.8	265	448	26.3	272	451	23.8
30	279	452	25.5	279	451	27.5	277	445	24.2

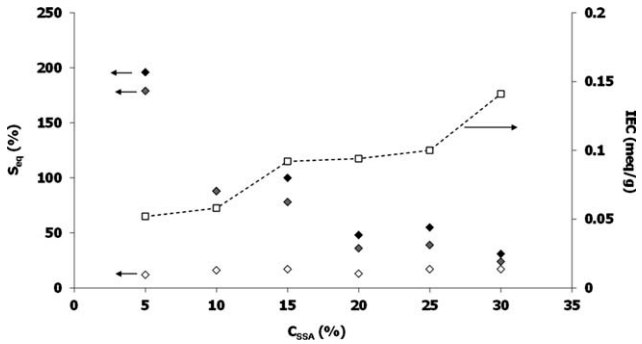

Figure 11 Ion Exchange Capacity (□, IEC) and swelling at equilibrium (S_{eq}) and as a function of the SSA composition of the PVA96hyd membranes submitted to heat treatment: Samples submerged in water (◇), water/methanol mixture (◈) and methanol (◆).

binary mixtures, the absorption of methanol seems to be unaffected by the composition of the membranes. This behavior suggests that, in general terms, the formation of a higher crosslinked structure and the removal of the OH groups can inhibit the transport of H_2O.[14] On the other hand, as it was expected, there is an increase on the IEC values at higher SSA concentrations, due to the presence of more sulfonic residues acting as ionic conducting sites.

The study of the transport properties of the PVA96hyd membranes were completed by the tests performed in DMFC monocells. The power curves (P = I–V), obtained from the polarization curves (I–V) are shown in Figure 12. The results show how the composition of the PVA-SSA membranes affects their behavior. The power curves were fitted to a second order function and the maximum power provided for each membrane (P_{max}) was also calculated (inlet in Fig. 12). According to these results, it is clear that the presence of higher SSA concentrations leads to improved performance of the monocells, possibly by the presence of more sites for proton conduction (see IEC values). However, we found that such improvement seems to have a maximum at SSA contents of around 25% of SSA (P_{max} = 299 mW cm^{-2}).

TABLE VII
Results from the Solvent Absorption and Ion Exchange Capacity of the *PVA96hyd* Membranes Submitted to Heat Treatment

	S_{eq} (%)			
C_{SSA} (wt %)	H_2O	H_2O/CH_3OH (8 wt %)	CH_3OH	IEC (meq g^{-1})
5	196	179	12	0.052
10	88	88	16	0.058
15	100	78	17	0.092
20	48	36	13	0.094
25	55	39	17	0.100
30	31	24	17	0.141

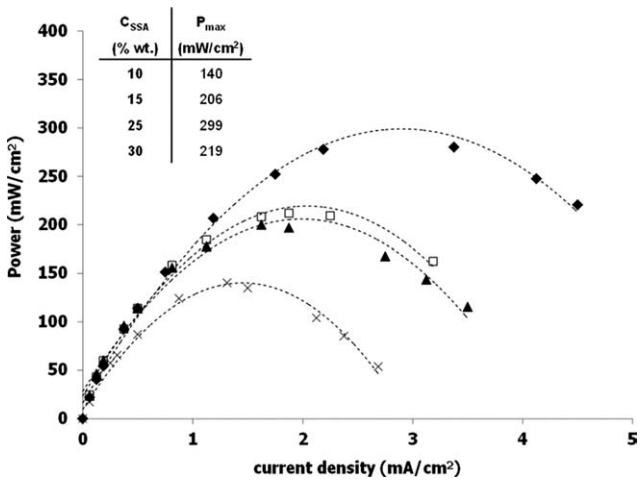

Figure 12 Results from the DMFC tests of the PVA96hyd membranes on the DMFC monocells. Power curves and maximum power obtained for: (x) PVA96hyd10%, (▲) PVA96hyd15%, (◆) PVA96hyd25%, (□) PVA96hyd30%.

CONCLUSIONS

The hydrolysis degree of the PVA substrate is significant in determining the structure and properties of PVA-SSA membranes prepared by a thermally accelerated esterification crosslinking reaction. The esterification of the PVA hydroxyl groups by the SSA carboxylic acid groups was observed in all the membranes studied and led to a crosslinked structure having enhanced thermal stability. The esterification reaction was found to occur even at room temperature and was accelerated by thermal treatment.

The PVA-SSA membranes with the higher hydrolysis degrees (PVA99hyd and PVA96hyd) showed the greater changes in properties post thermal treatment and also the greatest dependence on SSA concentration. The presence of tightly bound water in the PVA-SSA membranes was observed. The highest values of water content were seen for the membranes prepared using a PVA substrate with a hydrolysis degree of 96%, and this also exhibited the best processing properties in terms of the preparation of crosslinked PVA membranes. Membranes with intermediate concentration of sulfonic groups seems to be more appropriated for their use in DMFC, possibly by a combination of sufficient sites high proton conduction without considerable decrease on the water to methanol selectivity.

References

1. Blomen, L. Fuel Cell Systems; Plenum Press: New York, 1993.
2. Hoogers, G. Fuel Cell Technology Handbook; CRC Press: Nueva York, 2003.
3. US Department of Energy. Handbook of Fuel Cells, 5th ed.; EG&G Services: Morgantown, West Virginia, USA; 2000.
4. DeLuca, N. W.; Elabd, Y. A. J Polym Sci B Polym Phys 2006, 44, 2201.

5. Pivovar, B. S.; Wang, Y.; Cussler, E. L. J Membr Sci 1999, 154, 155.
6. Elmér, A. M.; Jannasch, P. J Polym Sci 2006, 44, 2201.
7. Kang, M. S.; Kim, J. H.; Won, J.; Moon, S. H.; Kang, Y. S. J Membr Sci 2005, 247, 127.
8. Rhim, J. W.; Lee, S. W.; Kim, Y. K. J Appl Polym Sci 2002, 85, 1867.
9. Chiellini, E.; Corti, A.; D'Antone, S.; Solaro, R. Prog Polym Sci 2003, 28, 963.
10. Yang, C. C.; Chiu, S. J.; Chien, W. C. J Power Sources 2006, 162, 21.
11. Kim, D. S.; Guiver, M. D.; Nam, S. Y.; Yun, T. I.; Seo, M. Y.; Kim, S. J.; Hwang, H. S.; Rhim, J. W. J Membr Sci 2006, 281, 156.
12. Socrates, G. Infrared and Raman Characteristic Groups Frequencies; Wiley: England, 2001.
13. Rhim, J. W.; Yeom, C. K.; Kim, S. W. J Appl Polym Sci 1998, 68, 1717.
14. Rhim, J. W.; Park, H. B.; Lee, C. S.; Jun, J. H.; Kim, D. S.; Lee, Y. M. J Membr Sci 2004, 238, 143.
15. Lin, C. W.; Huang, Y. F.; Kannan, A. M. J Power Sources 2007, 164, 449.
16. Mansur, H. S.; Oréfice, R. L.; Mansur, A. A. P. Polymer 2004, 45, 7193.
17. Xiao, S.; Huang, R. Y. M.; Feng, X. J Membr Sci 2006, 286, 245.
18. Hallinan, D. T., Jr.; Elabd, Y. A. J Phys Chem B 2007, 111, 13221.
19. Lee, J.; Lee, K. J.; Jang, J. Polym Test 2008, 27, 360.
20. Huang, Y. F.; Chuang, L. C.; Kannan, A. M.; Lin, C. W. J Power Sources 2009, 186, 22.
21. Kim, K.-J.; Lee, S.-B.; Won Han, N. Polym J 1993, 25, 1295.
22. Kang, M.-S.; Choi, Y.-J.; Moon, S.-H. J Membr Sci 2002, 207, 157.
23. Carretta, N.; Tricoli, V.; Picchioni, F. J Membr Sci 2000, 166, 189.
24. Zundel, G.In The Hydrogen Bond;Schister, P., Zundel, G., Sandorf, C., Eds.; North Holland Publ. Co.: Amsterdam, 1979; p 655.
25. Tury, A. Thermal Characterization of Polymeric Materials; Academic Press: San Diego, 1997; Vol. 1.
26. Qiao, J.; Hamaya, T.; Okada, T Polymer 2005, 46, 10809.
27. Ding, J.; Chuy, C.; Holdcroft, S. Chem Mater 2001, 13, 2231.
28. Kim, D. S.; Park, H. B.; Rhim, J. W.; Lee, Y. M. Solid State Ionics 2005, 176, 117.
29. Pandey, L. K.; Saxena, C.; Dubey, V. J Membr Sci 2003, 227, 173.
30. Carretta, N.; Tricoli, V.; Picchioni, F. J Membr Sci 2000, 166, 189.